

Enabling Ultra-Fine Pitch Packages: Soldermask Patterning using Laser Ablation

John Davignon and Jeff Howerton
Electro Scientific Industries
Portland, OR

William Alger, Gary Brist and Gary Long
Intel Corporation
Hillsboro, OR

Abstract

The trend towards tighter pitch, smaller features, and shrinking pad sizes have put a strain on the standard photolithographic processes for soldermask patterning on substrate packaging and rigid Printed Circuit Boards (PCB). These constraints have limited the ability of the package/board designer to shrink features and have resulted in yield losses by the fabricators. To date, the answer to this situation has been to re-capitalize with expensive Laser Direct Imaging (LDI) systems or modified semiconductor step and repeat equipment. This paper discusses direct laser ablation of soldermask as an alternative technology to enable fabricators to achieve very tight soldermask feature control.

Presented in this paper is the process and performance evaluation of the direct laser ablation process on soldermask for very fine pitch package placement on printed circuit boards. Results of solder adhesion, pre-surface finish pad morphology, and solder joint reliability to shock, bend, and thermal cycling are reviewed across design and process parameters. The evaluation looked at fabrication process variations across different soldermask types and soldermask thicknesses. Design implications between soldermask defined pads, metal defined pads and via in pad when used with soldermask direct laser ablation were also investigated.

Introduction

The breakout routing and pad sizes for fine pitch packages are determined by the trace/space and the soldermask feature tolerances of the industry. In mainstream PCBs for desktop and servers, the soldermask feature capability lags the trace/space capability and as a result is a greater limiter to breakout routing. See Figure 1. Equation 1 relates the requirements and trade-off between trace/space capability and soldermask capability. Using Equation 1 and applying it to different package pitch and bond pad sizes, it is shown that unless soldermask capability is less than +/-1.5mil (+/-38micron) it is impossible to route 0.4mm packages without trace feature less than 2mil (50microns).

With large format film and material movement, the industry capability for registration of a soldermask opening in relationship to a solder pad is between +/-2 (+/-50micron) and +/-2.5mils (+/-65microns). See Figure 2. In ultra -fine pitch packages, this level of soldermask registration and feature control prevents any routing on outerlayers. It also limits package pitches to roughly 0.6mm with single track 4mil traces and 10mil bond pads.

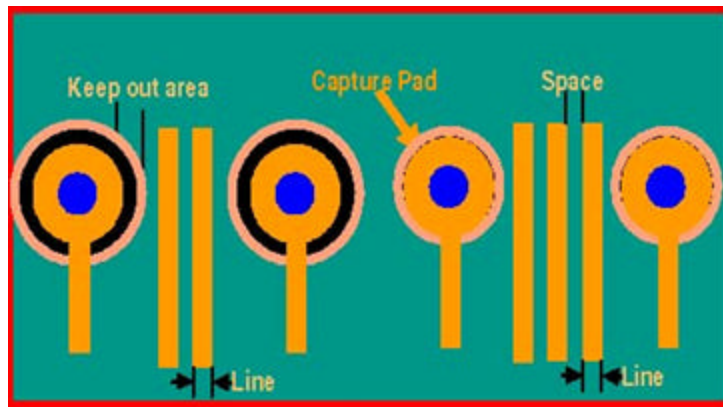


Figure 1 - Soldermask vs. Image Constrained Routing

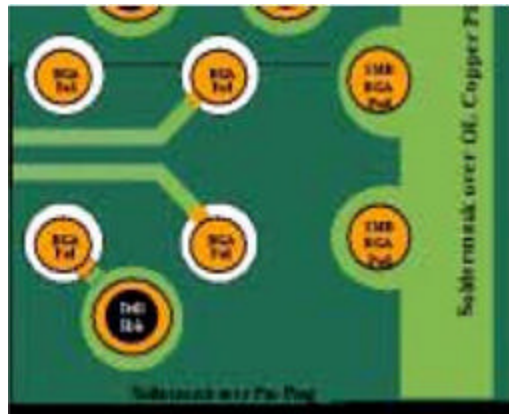


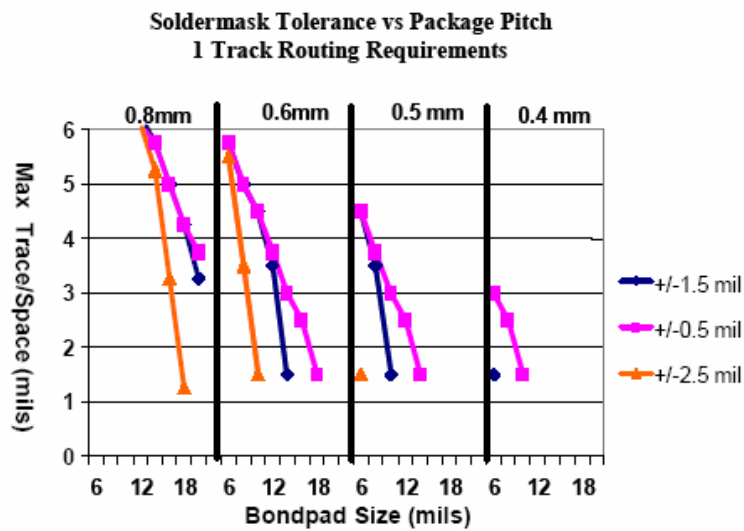
Figure 2 - Metal vs. Soldermask Defined Pads

Soldermask Positional Accuracy + Size Tolerance =

$$\pm \frac{\{\text{Pad Trace Space} + \text{Encroachment Allowance} - 2 \times \text{Max Etch Tolerance}\}}{2}$$

(1)

See Figures 3 and 4.



Simulations based on 2*Etch Tolerance Encroachment <0.5mils
Figure 3 – Routing/Bond Pad Trade-Offs

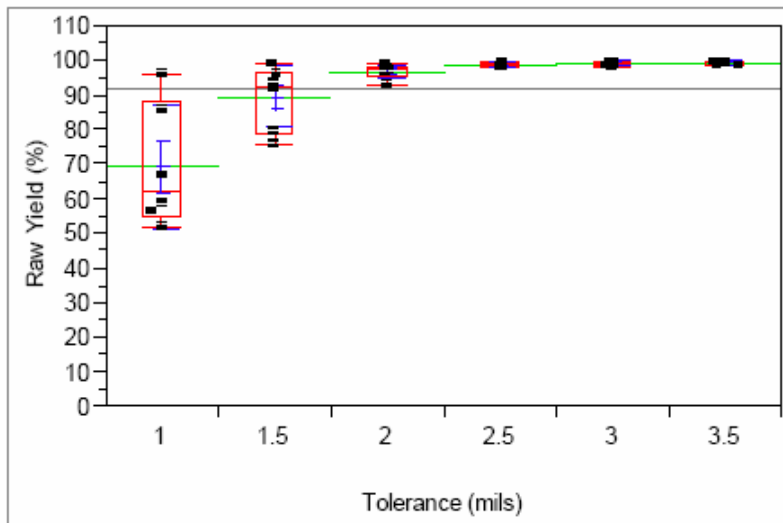


Figure 4 - Industry Mainstream Soldermask Capability (Intel Rev2 Industry Test Board)

The advantage of laser ablation of soldermask is two fold. First the registration and size tolerance is significantly better than the existing industry soldermask capability. Secondly, laser ablation can be applied selectively to panels. With laser ablation, metal defined soldermask openings can be fabricated that are only a few microns larger than the pad itself. See Figure 5. And by selectively using laser ablation in tight tolerance regions of a PCB, the cost of conversion and ownership of laser ablation equipment is reduced for the PCB fabricator. This makes it an appealing technology to enable needed soldermask capability within the industry.

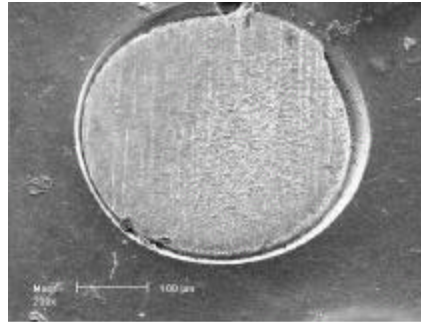


Figure 5 – Metal Defined Pad using laser Ablation of Soldermask⁵

Previous publications have documented the positional accuracy and feasibility of using lasers to pattern soldermask. The work outlined in this paper presents a look into the process window for laser ablation of soldermask at the PCB fabricator and the impact of laser ablation on the second level interconnect, package to PCB solder joint reliability. This work spanned several test vehicles, fabrication conditions, laser process parameters, and reliability metrics.

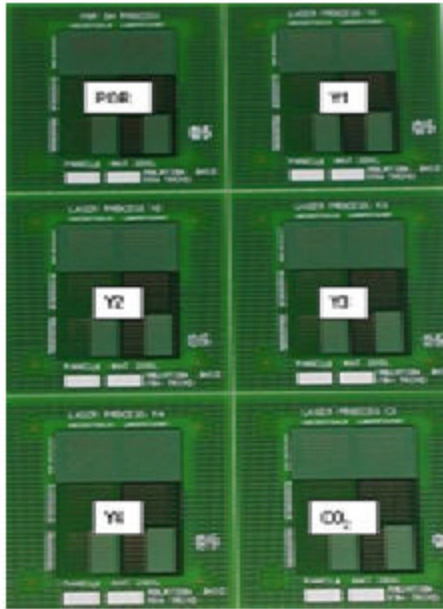
Manufacturing Feasibility

The manufacturing feasibility test board was designed to compare the cold ball pull and shear strength of BGA ball joints across different conditions of soldermask type, soldermask thickness, laser type, laser process settings and BGA pad designs. See Table 1. For each condition, the analysis of the ball to pad solder interface using laser ablation was compared to the standard print and develop process (POR – process of record) to help understand the feasibility and impact of each process setting and material selection.

Table 1 - Manufacturing Feasibility Parameters

Parameter	Values
Board Material	FR4 and RCC – Outer Layers
Ball Sizes	300 μm, 250 μm, 200 μm
Ball Comparison	Sn63/Pb37, Sn95.9/Ag4/Cu0.5
Soldermask Material	Supplier 1, Supplier 2
Soldermask Thickness	Thick, Thin
Pad Configuration	MOP, SMOP, uVIP, non-uVIP
Pad diameters (um)	350, 325, 300, 275, 250, 225, 200, 175, 150
Surface Finish	Immersion Silver

The test board was designed as a subpanel with six (6) coupons, one coupon for each of the soldermask patterning processes evaluated. The six soldermask processes were POR, CO2 laser and four different YAG laser processes. See Figure 6. The YAG laser processes were defined by four levels of ablation energy and used to evaluate the overall YAG process window and its interaction with different soldermask types and thicknesses. For a given soldermask material and soldermask thickness, the differing YAG laser processes resulted in different levels of melting of the copper pad surface. For the manufacturing feasibility study, subpanels were built using two material constructions. One construction consisted of a glass reinforced FR4 epoxy cap layer laminated to a standard glass reinforced FR4 epoxy core. The second consisted of a RCC (Resin Coated Copper) cap layer also laminated to a standard glass reinforced FR4 epoxy core. Each construction was then split across two soldermask materials and two soldermask thickness combinations. The thick soldermask condition was the result of a second soldermask coating.



Soldermask Patterning Process

1. **POR: Process of Record.**
2. **Y1: UVYAG (no Cu melting)**
3. **Y2: UVYAG (mild Cu melting)**
4. **Y3: UVYAG (moderate Cu melting)**
5. **Y4: UVYAG (heavy Cu melting)**
6. **C1: CO₂ process**

Figure 6 – Manufacturing Feasibility Subpanel⁵

Each coupon within the subpanel contains multiple design combinations. See Figure 7. These include soldermask defined pads on a ground plane and metal defined pads. Both pad types also contained uVIP (microVia In Pad) and non-uVIP conditions. The non-uVIP and metal defined pads provided the standard dogbone pattern of via pad connecting to ball pad by a short trace. In addition, the lower 1/3rd of the coupon was reserved for experiments in soldermask taper profiling. See Figure 8.

Each coupon (see Figure 7) had 27 rows and each row had 20 pads. The 20 pads were identified with column designators: A, B, C, D, E, F, G, H, J, K, L, M, N, P, R, T, U, V, W, Y. Rows 1-9 were solder mask defined pads (SMDP) with row 1 being the 350um pad diameter and decreasing to 150um on Row 9. Rows 10-18 were metal defined pads (MDP) and followed same pad diameter format as SMDP. And rows 19-27 were a combination of MDP and SMDP, the pads A, B, C, D, E, L, M, N, P, R were MDP and pads F, G, H, J, K, T, U, V, W, Y were SMDP.

Columns A, B, C, D, E, F, G, H, J, K are microvias in the pad (uVIP) and columns L, M, N, P, R, T, U, V, W, Y are non uVIP pads with a short trace.

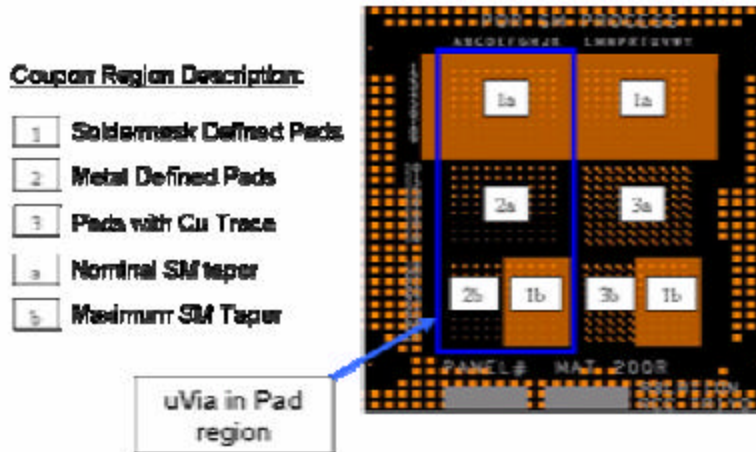
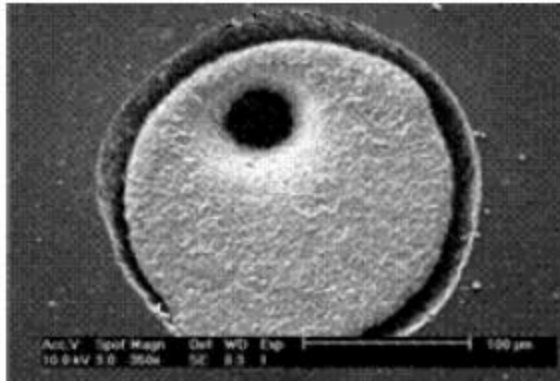
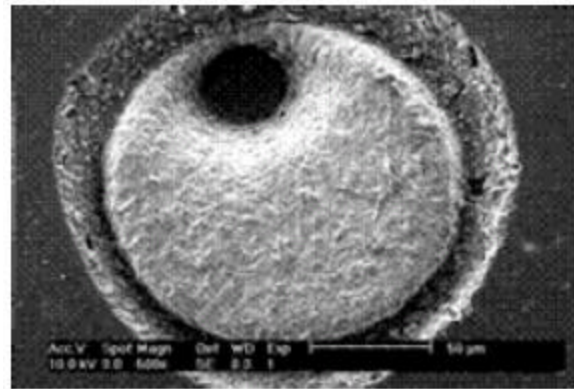


Figure 7 - Coupon Detail⁶



Nominal Taper



Maximum Taper

Figure 8 - Ablated Pads with Microvia⁵

Mechanism of UV Laser Soldermask Ablation

When a laser beam irradiates a target material, the photons are absorbed through interactions with the valence electrons in molecules or atoms, causing these electrons to move from ground to excited states. When the laser fluence is high enough, detectable changes in material can occur, such as phase transformation or material removal. There are primarily two processes that occur in the UV laser material interaction, i.e., photochemical ablation and photothermal ablation.

Of all the electronic materials encountered in laser micro-via drilling applications, polymers interact with UV photons mainly through photochemical ablation, however, there is evidence indicating that a photothermal process is partially involved. In order to obtain a perfectly clean via free of debris it is expected that the materials are all driven rapidly through the melt phase and into the vapor phase prior to expulsion from the interaction zone by the gas dynamic effects.

Direct Laser Ablation of Soldermask

In direct laser drilling, no mask is required. Soldermask can be removed by way of punching, trepanning, or spiraling, see Figure 9, depending on whether the via size is equal or larger than the size of the beam. In punching mode, the size of the via is equal to that of the beam and the via is formed by direct pulsing a number of pulses on a same location. For vias with diameters larger than that of the beam, the laser beam moves either in a circular trajectory (“trepanning”) or outward from the center in a spiral (“Spiraling”). To achieve a high enough beam placement accuracy and ablation throughput, a high-performance beam positioning system needs to be implemented to achieve extremely precise and fast movement of the beam spot in direct laser drilling.

Depending on the specific drilling applications, the laser beam profile can take the form of Gaussian, clipped Gaussian, and ‘top hat’ like shaped and imaged beam. The ablation of soldermask is best processed using a shaped and imaged beam. This technique spreads out the energy found in a Gaussian beam and flattens the top of the beam to give a larger uniform energy distribution. See Figure 10 for pictorial description of a shaped beam. This allows the fabricator to develop process parameters that are above the ablation threshold (energy density) of the soldermask and still below the ablation threshold of the copper pad. This allows for optimal removal of the soldermask without damage to the underlying copper surface.

The ‘top hat’ like beam profile can be accomplished by specially designed optics. Figure 11 is the schematic of the optical path for beam shaping and imaging that has been used on ESI laser drilling systems, where the Gaussian beam profile, after going through the beam shaping optics, is transformed to a near-uniform “top hat” profile at the plane of the aperture.

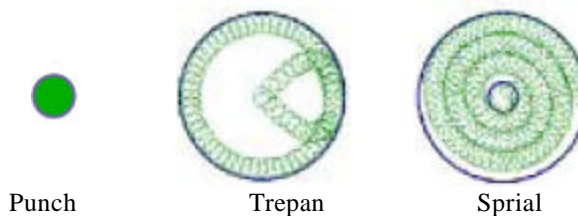


Figure 9 - Soldermask Removal Formation Techniques

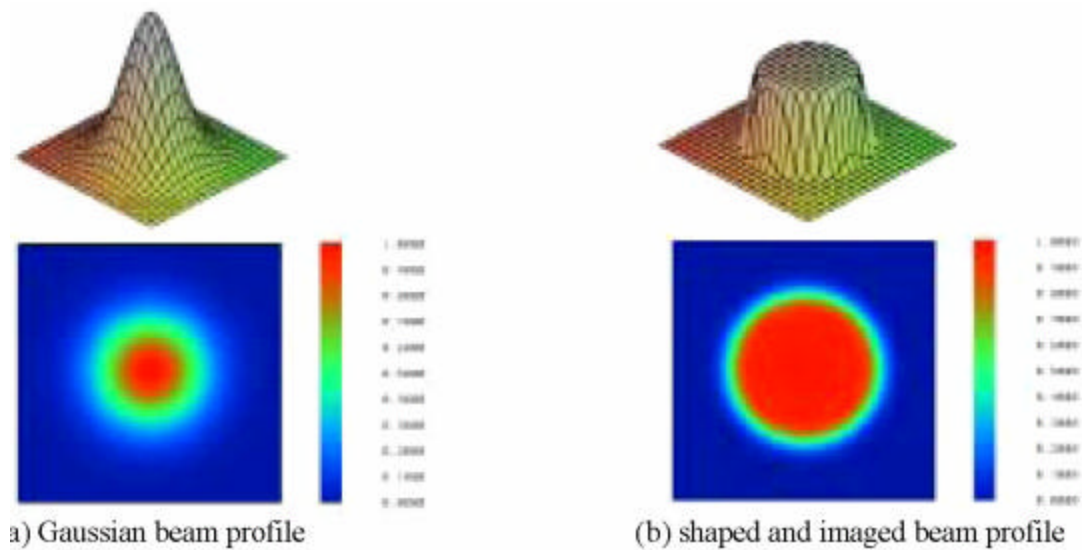


Figure 10 – Beam Shapes

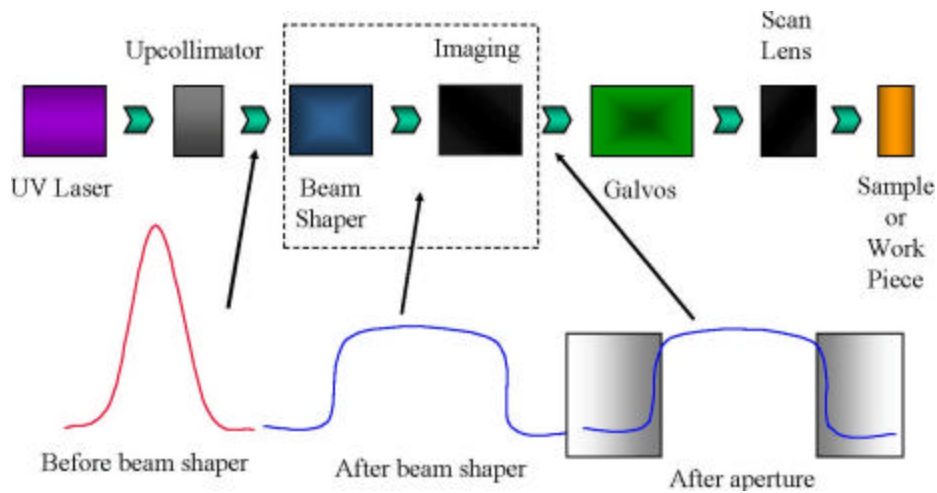


Figure 11 – Optical Path for Beam Shaping

Although UV lasers are very efficient at removing copper, the process can be developed that will efficiently remove soldermask without damaging the underlying copper pad. Figure 12 shows a copper pad with the soldermask removed. Notice the scratch mark on the copper surface and under the soldermask, this is visual evidence that the copper pad has not been damaged by the removal of the soldermask using the UV laser process.



Figure 12 – Example of No laser Alteration of Copper Surface by UV Laser Processing⁵

As mentioned earlier the test matrix was designed to give 4 different levels of copper surface damage to assess the process robustness. The copper damage levels were artificially induced into the copper surface by increasing the energy density in the shaped beam to the point where it started to melt the copper surface. The next section discusses the effect of the different levels. The soldermask thickness variations were handled by modifying the velocity of the beam so that the bite size or overlap of each pulse resulted in putting more energy in the via. This increase in energy results in a higher ablation rate and allowed the thicker soldermask to be efficiently ablated.

The variation in taper was handled by modifying the imaged beam profile so that a less straight sidewall was produced. This method allows for a reasonably controlled taper profile based on the thickness variation of the soldermask.

Solderability

As subpanels were processed, the soldermask was first ablated and then immersion silver was applied as a surface finish prior to being shipped for assembly. The BGA pads of each subpanel were evaluated to note changes in copper topography and detect potential residue on the pad surfaces. The evaluation was done at three locations in the manufacturing process flow. First was immediately after laser ablation. Second was after the micro-etch of the immersion silver line. And third was after immersion silver coating. In fabricating the subpanels, they were first processed with the POR which only patterned the upper left coupon and then processed through each laser ablation process to pattern the corresponding coupon.

After the laser ablation process, it was easy to see the differences between the four different YAG laser processes and the progressive melting of the copper pad surface at progressively higher ablation energies. See Figure 13. Also noticeable was the presence of a dark film or residue remaining on the pads in the C1 coupon which was processed using CO2 laser. After the micro-etch of the immersion silver process, the subpanels were inspected and found that the micro-etch removed most of the variation in the copper topography that existed across the YAG laser processes and that the YAG laser processes were close in roughness and coloration to the POR process. After the micro-etch, it was still evident that a film or residue still remained on the pad in the C1 coupon. This was visually evident by the mottled or darker regions on the CO2 (C1) ablated pads. After the immersion silver process, the contrast on the CO2 pads was further heightened as the copper under the film or residue remained a copper color. After the immersion silver process the distinction between POR, Y1, and Y2 were not quantifiable. Y3 and Y4 also appeared to be very similar in texture yet distinct from Y1 and Y2.

The surface analysis showed the contamination on the CO2 (C1) process pads that was present after ablation and remained on the pad through the micro etch process and resulted in an incomplete coverage of the pad by the immersion silver finish. The lower ball attach rate on the CO2 pads during the ball attach process was attributed to the presence of residual contamination on the C1 process pads.

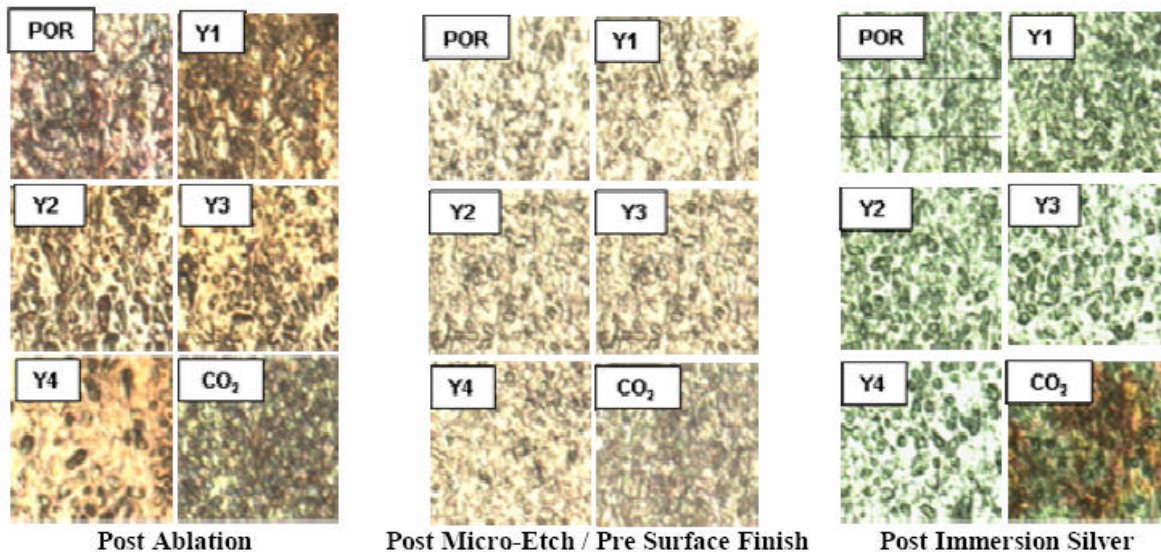


Figure 13 - Copper Pad Topography by Ablation Process⁵

Following immersion silver, the panels were shipped to assembly for ball pull and ball shear testing. At assembly, 300um balls were attached to the 300um and 250um pads. These balls were attached with a ball shooter.

Ball Attach Methodology

For the initial ball pull and ball shear testing, 300um balls were placed on the 300um and 250um pads. The 300um balls were placed on the coupon with a PAC Tech Solder Ball Bumper. In some of the tests, balls were heated to the reflow temperature with the integrated laser prior to shooting the ball on the board. The rest of the tests were done by shooting the ball on to the coupon with flux and placing the coupon in a reflow oven. The shoot and reflow process came closer to replicating the standard reflow process for packages, then the laser method. The same attach methods were used for leaded (Sn63/Pb37) and lead free (Sn95.5/Ag4/Cu0.5) balls.

Cold Ball Pull and Shear Tests

A Dage 4000 machine was used to perform the cold ball pull and ball shear tests. All of the tests were done with a 300um diameter ball attached to 300um and 250um MDP, SMDP, non uVIP and uVIP pads. Tests were performed under the same conditions.

Results indicate the solder joint strength of the laser ablated pads is comparable to the strength of the POR pads. Laser processes resulted in lower shear forces than POR process but also resulted in higher pull forces than POR process. See Figure 14. This was the result of the differences in ball geometries and proximity of soldermask to the attached ball. See Figure 15. The non uVIP solder joints performed better than the uVIP solder joints, which from cross section analysis, was attributed to the reduced ball attach area due to the voiding caused by the microvia. Soldermask defined pads exhibited similar results for cold ball pull and ball shear.

The interaction between the ablation processes and lead free assembly processing was also investigated. Figure 18 shows the results of ball pull strength between standard SnPb solderballs and SnAgCu, Pb-Free, solderballs across various UV YAG ablation processes for 300um pads in thin supplier 1 soldermask. For the POR, Y2, and Y3 processes, the Pb-Free solderballs had slightly lower pull strength; but, was not statistically significant. Similar results were obtained across the other soldermask parameters and pad sizes for both ball pull and ball shear. Again, the solder joints of balls attached to pads formed by ablation performed as well as balls attached to pads formed by the POR process. No interaction with lead free assembly was noted.

The cold ball pull and ball shear data for the CO₂ (C1) process coupon, for which the balls successfully attached, was almost identical to the YAG laser process data. As mentioned previously, the CO₂ process pads had a residue/film remaining after the immersion silver and experienced a significant amount of ball attach failures. What can be gathered from this portion of the testing is that when ball attach was successful on pads ablated with CO₂, the resulting adhesion was good and the joint was not degraded.

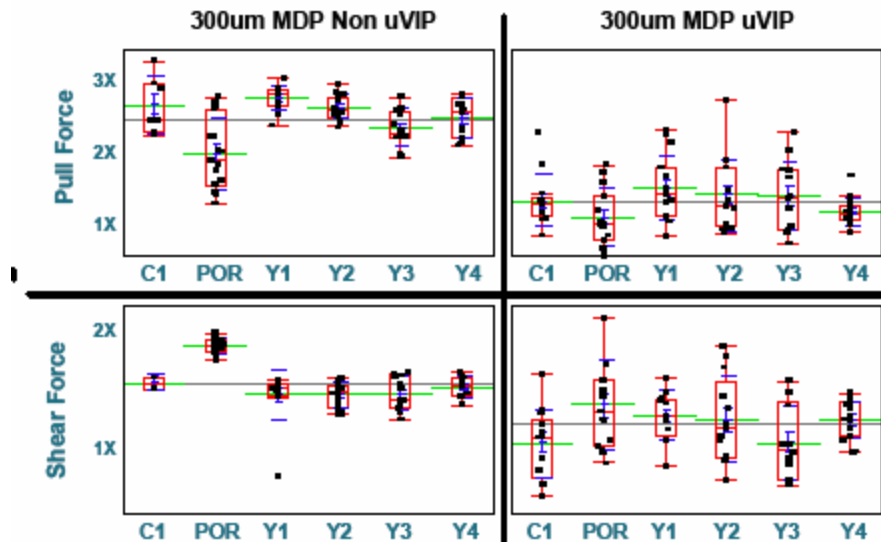
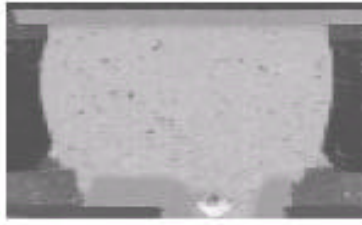
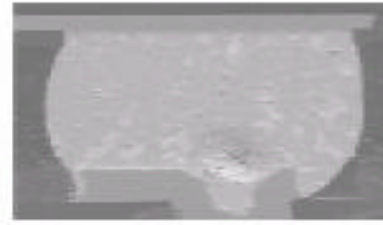


Figure 14 – Test Data for 300um Sn63Pb37 Balls on FR4 Board Material



Laser Ablation: Soldermask close to pad with solder wetting partially down pad sidewal



Photoimaging and Develop: Soldermask developed away from pad with solder wetting down to foot of pad

Figure 15 – Physical Differences⁶

Manufacturing Parameters and Material Results

A key outcome of the testing was to determine any impact, if any, of manufacturing parameters and material selection on the process window of the laser ablation process. The impact of soldermask processes was tested using two soldermask materials and two soldermask thicknesses. Figure 16 shows the comparison of the normalized ball pull and ball shear data from 300um metal defined pads using the UV YAG ablation across the different soldermask parameters. No significant differences were noted. This indicated that the ablation process has a wide process window for dealing with varied soldermask processes. Similar results were obtained for the other pad sizes as well as for the POR process.

The other material interaction tested was between boards using RCC under the outerlayer copper and boards using glass reinforced FR4 under the outerlayer copper. The data indicated that there was no interaction between the ablation processes and these two materials when comparing the ball pull and ball shear results. Data also indicated that the solder joints formed on pads formed with ablation processes performed as well as solder joints on pads formed with the POR process.

As expected, there were differences in both ball pull and ball shear strength across different pad / ball geometries. In all cases laser ablation of the pad did not compromise the integrity of the solder joint. Figure 14 shows that VIP, pads with microvias located within the solder pad, had lower ball pull and ball shear strength than the non-VIP solder joints. Figure 17 shows the ball pull strength for solder joints of pads on FR4 formed in thick supplier 1 soldermask. The results show that the pull strength of the 250um pad was about 10% less than the pull strength of 300um pads. This correlated to the reduced cross sectional area of the solder joints formed on the 250um pads. In addition, balls on soldermask defined pads had lower pull strength than balls on metal defined pads. These results were consistent across the different soldermask parameters, ball composition, and board material. In all cases, the pull strength of balls on pads formed by laser ablation performed as well as balls on pads formed with the POR process. The results from the shear strength data showed the same interaction with pad / ball geometries.

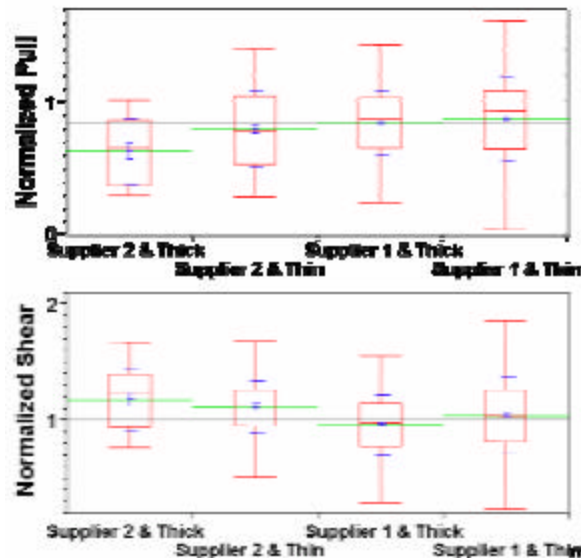


Figure 16 - 300 MDP by Soldermask Parameters

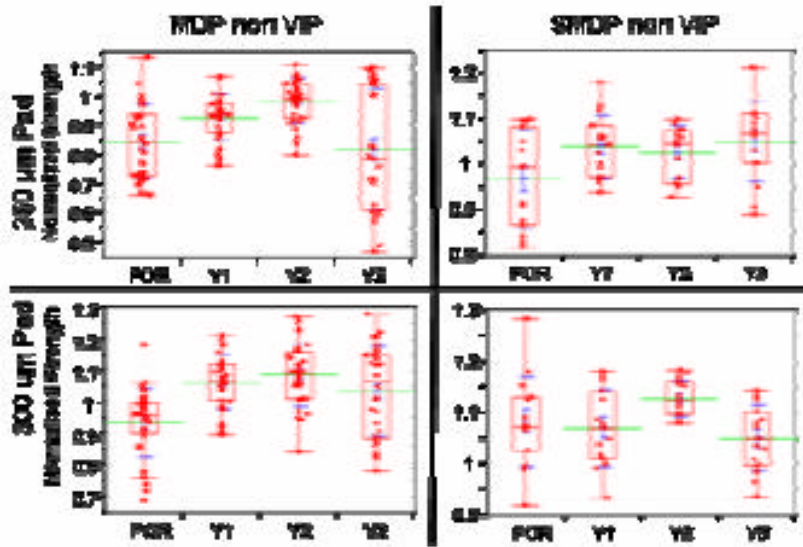


Figure 17 – pad Geometry Interactions on FR4 Board with Thick Soldermask Supplier 1

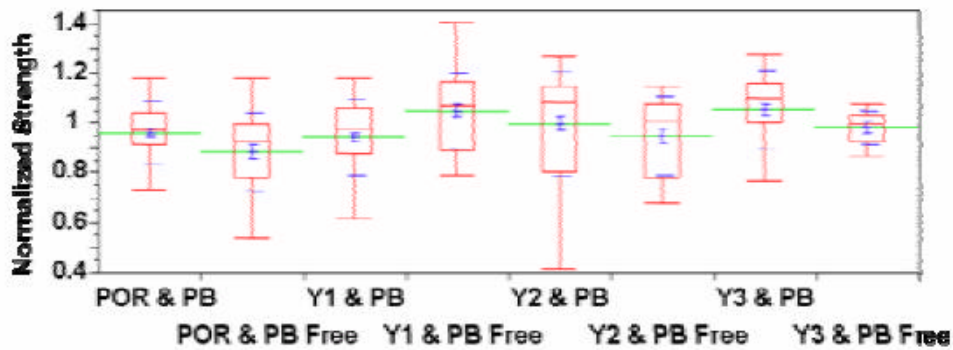


Figure 18 – Comparison by Ball Composition on Ball Pull of 300um pads, Thin Soldermask Supplier 1

Package/Assembly Reliability

Comparison of package/assembly reliability between the six soldermask patterning processes used in the manufacturing feasibility study consisted of shock and bend testing as well as thermal stress cycling. A single board design was used for the shock and bend testing. The shock and bend testing and the associated board design were done in accordance with JEDEC standard JESD22-B111, “Board Level Drop Test Method of Components for Handheld Electronic Products”. The thermal stress test board was a daisy chain design and sized to fit into a 6 inch HATS (Highly Accelerated Thermal Shock) chamber manufactured by ITRS. In all cases the laser process results were baselined to the POR process results to help understand the net reliability impact of the lasered pads. The test population was at a screening test level.

The test boards were designed with 300um metal defined pads and 125 um microvias on the top side of the board and metal defined pads without microvia on the bottom side. The board material was FR4 with an immersion silver surface finish. The test boards were divided between four soldermask patterning processes. The four solder mask patterning processes selected were the POR, Y1, Y3, and C1 processes used in the manufacturing feasibility testing.

Thermal Stress Test

The thermal stress test board (See Figure 19) was assembled on the top side, metal defined uVIP pads, with 4 nets and 8 daisy chained packages. The design allowed a failed component to be jumpered, bypassing the failed component and allowing the testing to be continued on the 2nd package. The temperature cycle was set at -40 C to 125 C. At 500 cycles no components had failed except for the packages assembled to the pads ablated with the C1 process. For the thermal stress test boards processed with the C1, or CO2 laser process, 50% of the packages were open immediately after assembly (reflow) and the remaining failed within 10 thermal stress cycles. Again, this corresponded with the C1 results of lower ball attach rate and evidence of a remaining film preventing full coverage of the immersion silver surface finish on the pads. At 500 thermal cycles the POR and Y1, Y3 did not show difference in ball joint integrity.

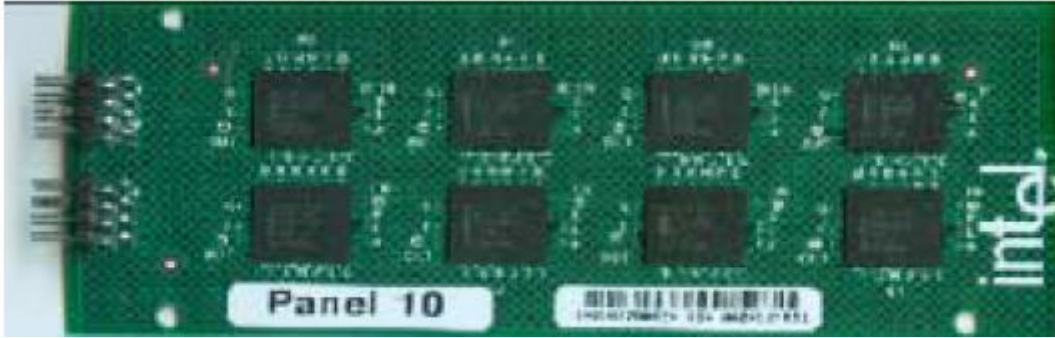


Figure 19 – Thermal Stress Board⁶

Shock Reliability Test

The shock board (See Figure 20) had 5 daisy chained packages assembled to the board. In accordance with JESD22-B111, the boards were subjected to a 1500G level drop and were cycled until more than 50% of the packages on each board electrically failed.

Given the evidence that differences in ball shape due to proximity of the soldermask to the ball pad were influencing both the ball pull and ball shear results, the solder mask openings of each test board were created with the POR process. The pads on the test boards were then processes with the corresponding YAG process. This had the effect of altering the copper surface while maintaining a consistent soldermask opening around each pad. The result of this test showed the affect of the YAG laser processing on the solder joint without the confounding interaction of soldermask proximity and ball shape.

The YAG laser modified copper surfaces in this test resulted in higher shock cycles to failure than that of the POR process. See Figure 21. Cross section analysis of the POR, Y1 and Y3 solder joints where identical in dimensions and wetting of solder down along sides of the pad as shown in Figure 22. This result indicated that for a fixed ball/pad profile the YAG laser processes, Y1 and Y3, maintained or slightly improved the solder joint reliability when subjected to shock.



Figure 20 – Shock Reliability Test Board⁶

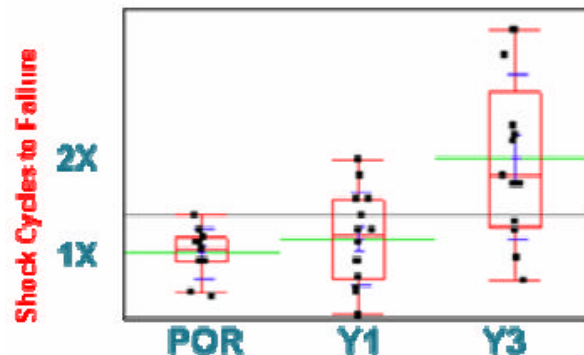


Figure 21 – Shock Cycles of Failure for MDP Non UVIP

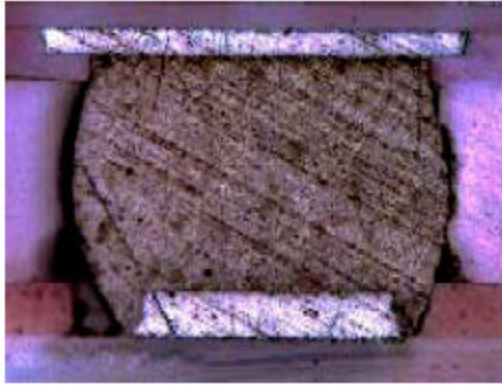


Figure 22 – Typical MDP Non uVIP Cross Section⁶

Bend Reliability Test

The bend test board had 9 daisy chained packages assembled to the board. See Figure 23. Each test board had packages on one side. The boards were subjected to a single displacement bend at 10,000 cycles per hour and they were cycled until at least 50% of the packages on each board electrically failed. Electrical failures were the result of opens due to ball cracks within the ball or cracks between the ball and pad surface.

Figure 24 shows the relative cycle to failure between packages attached to solder pads formed by the POR and Y1, Y3 UV YAG process. The YAG laser modified copper surfaces resulted in more shock to failure cycles than the POR process. Since the solder mask openings were created under the same conditions as the metal defined openings on the shock board, this bend data indicates that the lased pads with the modified surface results in a solder joint bond as strong or slightly stronger than the POR pads

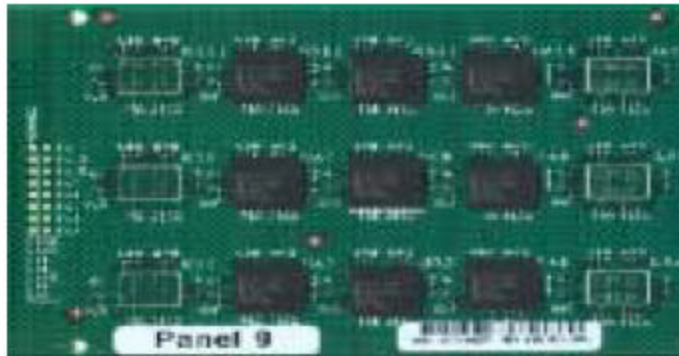


Figure 23 – Bend Test Board⁶

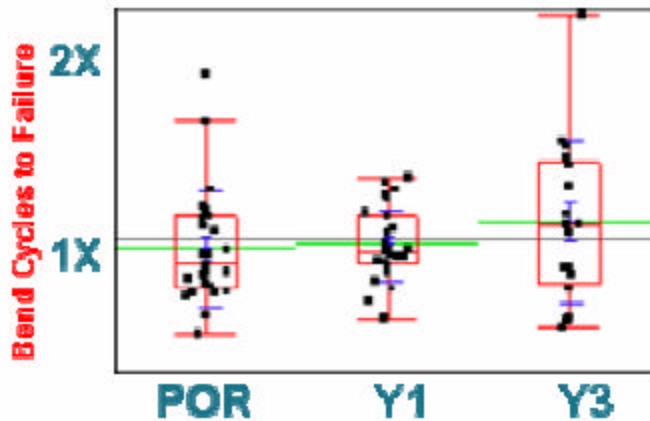


Figure 24 – Bend Failures for MDP

Summary

Laser Direct Ablation (LDA) of soldermask can improve solder mask registration on PCB's which allows the designer to use larger board features and/or more routing tracks under the BGA. This allows the utilization of higher density packages and smaller pitches, by improving the routing on the outer layer and assisting the reduction of layer count by removing the need for a large clearance area around the attachment pad. This helps the IC package designer, PCB designer, and PCB fabricator to build with fine pitch packages without incurring high capital cost.

Laser direct ablation of soldermask to form solder pads did not degrade solder joint integrity as seen in ball pull, ball shear, and package reliability testing. Solder joints on pads formed by laser direct ablation showed equivalent performance to solder joints on pads formed by the POR process. Laser ablation also demonstrated a wide process window in terms of acceptable laser processes across soldermask materials and soldermask process conditions. There were no differences noted between the laser ablation processes and POR process in terms of interaction with ball / pad geometries or pad designs.

Solder joint reliability testing of daisy chain packages also demonstrated good reliability for the laser direct ablation of solder mask. Bend and shock data showed no degradation compared to the POR process. The data showed that the copper pads with laser modified topography may even result in a solder joint strength better than the POR pads.

It is not recommended that CO2 process be used for soldermask ablation of solder pads without a secondary process to remove any residual residues or films. The data from the surface analysis, the lower attach rate and the early failure of the packages indicates solder joint reliability issues with the CO2 process as a result of remaining residues after ablation.

References

1. G. Brist, J. Davignon; "Alternative Technology for Soldermask and Primary Resist Patterning using Laser Direct Ablation" PCB West, (April 2003)
2. J. Davignon; "Processing High Density Boards with UV Lasers " Circuitree, October 2004
3. C. Vaucher, R. Jaquet; "Laser Direct Imaging and Structuring: An Update" Circuitree, August 2002
4. J. Davignon, Sudhakar Raman, "New Laser Capabilities to Enable New Design Improvements" Intel Technical Symposium, Sept 2003
5. Picture courtesy of ESI
6. Courtesy of Intel